

Effect of Zinc Maleate/Zinc Oxide Complex on Thermal Stability of Poly(vinyl chloride)

Guoxing Li, Ming Wang, Xingliang Huang, Haixia Li, Hong He

School of Chemistry and Chemical Engineering, Southwest University, Chongqing 400715, China

Correspondence to: M. Wang (E-mail: mwang@swu.edu.cn)

ABSTRACT: In this study, zinc maleate (ZnMA) and zinc oxide (ZnO) complex (ZnMA/ZnO) was prepared by two methods, namely, by the reaction of maleic acid (MAH) with excess ZnO in aqueous solution and by direct mixing of ZnMA and ZnO at 180°C. The chemical structure of the complex was analyzed by X-ray diffraction, thermogravimetric analysis (TGA), and Fourier transform infrared (FTIR) spectroscopy. The thermal stabilizing effect of the complex on poly(vinyl chloride) (PVC) was evaluated through static and dynamic stability methods. Compared to calcium and zinc soaps and ZnMA alone, the complex exhibited better thermal stabilizing effect on PVC. The stabilization mechanism was also investigated by ultraviolet–visible spectrometer, FTIR, TGA, and gel content analysis. The results indicated that the complex which involved the replacement of labile chlorine atoms hindered the formation of conjugated double bonds in PVC chains via Diels–Alder reaction, and ZnMA/ZnO complex also exhibited the ability to absorb hydrogen chloride. © 2014 Wiley Periodicals, Inc. *J. Appl. Polym. Sci.* **2015**, *132*, 41464.

KEYWORDS: degradation; poly(vinyl chloride); thermal properties

Received 29 April 2014; accepted 29 August 2014

DOI: 10.1002/app.41464

INTRODUCTION

Poly(vinyl chloride) (PVC) is one of the most important polymeric materials which is extensively used in numerous fields such as water pipes, window profiles, house siding, wire cable insulation, and flooring. It exhibits superior mechanical and physical properties, high chemical and abrasion resistance, non-flammable nature, good performance, and it is relatively cheap.¹ However, PVC can easily undergo degradation which leads to release of hydrogen chloride (HCl) during its processing resulting in loss of some properties. The loss of HCl from the chains develops sequences of conjugated double bonds leading to several colorations of the polymer. The color changes from white to yellow, brown, and finally black. The mechanical and physical properties simultaneously degrade significantly.² Appropriate stabilizers can inhibit the degradation of PVC during its thermal processing. Therefore, to expand the area of application of PVC, it is necessary to add thermal stabilizer to prevent it from degradation.

In practice, several thermal stabilizers are used to retard the degradation of PVC, such as lead salts,³ organic tin,⁴ soap salts,⁵ and rare earth compounds.⁶ The stabilization mechanism of the above mentioned stabilizers can be summarized as follows^{7–9}: first, preventing the formation of conjugated double bonds by replacing the labile chlorine atoms in PVC chains, second, restraining the self-catalytic dehydrochlorination through the

absorption of HCl. However, most of the stabilizers, in particular, the lead salts are toxic and will be eliminated in the future.

Therefore, highly efficient, relatively cheap, and environmentally friendly innocuous stabilizers have been given significant attention to overcome the abovementioned drawbacks. In particular, mixture of calcium stearate (CaSt₂) and zinc stearate (ZnSt₂) are innocuous thermal stabilizers because of good synergistic effect between them.^{10–12} However, an undesirable product, zinc chloride (ZnCl₂), is formed in PVC thermally stabilized with CaSt₂/ZnSt₂, which catalyzes the degradation of PVC and results in a sudden “zipper dehydrochlorination.” Thus, novel highly efficient zinc-based stabilizers exhibiting negative catalytic effects on the degradation of PVC are highly desirable.

Recently, zinc barbiturate,¹³ pentaerythritol-zinc,¹⁴ basic zinc cyanurate,¹⁵ zinc glycerolate,¹⁶ zinc borate,¹⁷ and zinc dicarboxylates¹⁸ were synthesized and employed to improve the thermal stability of PVC. The above mentioned zinc salts exhibited obvious enhancement in thermal stability compared to ZnSt₂, and delayed or stopped the “zinc burning” during PVC processing. In our previous work, zinc maleate (ZnMA) was synthesized and its thermal stabilizing effect on PVC was evaluated.¹⁹ It was observed that the synergistic effect of ZnMA/CaSt₂ was significantly higher than that of CaSt₂/ZnSt₂ stabilizers. Thus, highly efficient ZnMA acted as an excellent thermal stabilizer for PVC and provided an alternative way for developing

extremely effective innocuous stabilizers. ZnMA not only replaced the labile chlorine atoms in PVC chains, but also interrupted the formation of polyene via Diels–Alder reaction.

In this study, a novel ZnMA/ZnO complex with more efficient thermal stabilizing effect than ZnMA was prepared by the reaction of MAH with excess ZnO, or directly mixing ZnMA and ZnO. The thermal stabilizing effect at different molar ratios of ZnO and MAH or ZnO and ZnMA was discussed and the optimal conditions for the preparation of ZnMA/ZnO complex were investigated. The thermal stabilization mechanism of the ZnMA/ZnO complex was further investigated and discussed along with their structures.

EXPERIMENTAL

Materials

The PVC used in this study was PVC-SG5 ($\eta = 114$, $K = 66$ according to the manufacturer) purchased from Yibing TianYun, Sichuan, China. ZnMA was synthesized by reacting MAH (Chengdu Kelong Chemical Reagent, China) with ZnO (Ningbo Daqiao Chemical Reagent, China), following the literature method.¹⁹ CaSt₂ was bought from Ningbo Daqiao Chemical Reagent, China.

Preparation of Stabilizer

First type of ZnMA/ZnO complex (represented as ZnMA-I) was prepared by adding ZnO in aqueous solution of MAH which was directly dried at 180°C to remove solvent after adequate reaction. The molar ratio of ZnO and MAH was selected in the range from 0.5 to 2.0 in order to obtain an optimal molar ratio for thermal stability of PVC. For comparison, second type of ZnMA/ZnO complex (represented as ZnMA-II) was obtained by directly mixing ZnO and ZnMA at 180°C in the molar ratio ranging from 0.2 to 1.5. Pure ZnMA was synthesized following the literature method.¹⁹

Measurements

To obtain the ZnMA-I and ZnMA-II stabilizers with optimal molar ratios, and to investigate the thermal stabilizing effect of the stabilizers, the static stability time of PVC with ZnMA-I or ZnMA-II as stabilizers was investigated by the congo red test at 180°C. The PVC and stabilizers with different weight ratios were dry-blended in a mixing machine, and approximately 20 g of the mixture was used for the test. The dynamic stability time was obtained by a Brabender plastograph (Plasticorder) mixer (Hapro RM-200). The PVC and stabilizers with different weight ratios were dry-blended in a mixing machine, and approximately 70 g of the mixture was employed for the test. The temperature of mastication was about 180°C, and the rotor rate was 30 rpm. The thermogravimetric analysis (TGA) was also performed to study the thermal stability of PVC with the optimal ZnMA-I and ZnMA-II stabilizers, respectively, and to investigate the structure of the complexes formed in the ZnMA-I and ZnMA-II stabilizers with optimum stability effect, at a heating rate of 10°C min⁻¹ from room temperature to 600°C under nitrogen flow (50 mL min⁻¹), by a TA Q600 analyzer. The samples were also dry-blended in a mixing machine before the TGA test.

Fourier transform infrared (FTIR) spectra of the above mentioned samples were obtained on a Nicolet 170SX (Madison, WI)

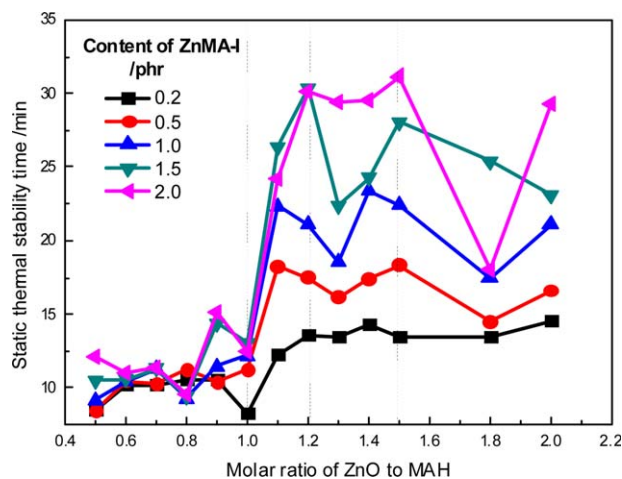


Figure 1. Effect of molar ratio of ZnO to MAH on static thermal stability for PVC with ZnMA-I. [Color figure can be viewed in the online issue, which is available at wileyonlinelibrary.com.]

by KBr disc method. Wide angle X-ray diffraction (WAXD) analysis was carried out on a MSAL-XD 3 (Beijing Purkinje General Instrument, China), using a Cu K α radiation with a wavelength of 1.54 Å (36 kV and 20 mA). Scanning was performed over the angle range $2\theta = 8\text{--}80^\circ$ with a scan rate of 4°/min.

To study the stability mechanism of the optimal ZnMA-I and ZnMA-II stabilizers, the FTIR experiments were performed with wavenumber ranging from 500 to 4000 cm⁻¹. The PVC/ZnMA-I and PVC/ZnMA-II samples after degradation with different time were dissolved in tetrahydrofuran (THF). The precipitate was filtered, dried, and then weighed as gel content; however, the soluble part was reprecipitated in deionized water to remove some residual complexes and then cast into ZnSe window cell for FTIR test. Ultraviolet–visible (UV–Vis) spectrophotometer (UV-2550, Shimadzu, Japan) was used to investigate the content of double bonds present in the PVC/ZnMA-I and PVC/ZnMA-II samples after degradation. The samples (0.01 g) were dissolved in THF (10 mL) by ultrasonication.

RESULTS AND DISCUSSION

Effects of ZnMA/ZnO Stabilizers on the Thermal Stability of PVC

The static stability time of PVC with different ZnMA-I prepared by controlling the molar ratio of ZnO to MAH was analyzed by the congo red method, which was related to the release of certain amount of acid gas from the samples. The effect of incorporation of ZnMA/ZnO complex on the static thermal stability of PVC can be divided into four different regions based on their molar ratios as shown in Figure 1. First, the static stability time of PVC/ZnMA-I samples maintains a low level, which is independent of the content of ZnMA-I, when the molar ratio of ZnO to MAH is below 1.0. Second, the static stability time improves abruptly with the increase in molar ratio of ZnO to MAH from 1.0 to 1.2. Thus, the improvement becomes more obvious with more content of ZnMA-I. Third, the static stability time acquires a high value when the molar ratio of ZnO to MAH increases from 1.2 to 1.5. This high value increases from about 12 min to 30 min with the content of ZnMA-I increasing

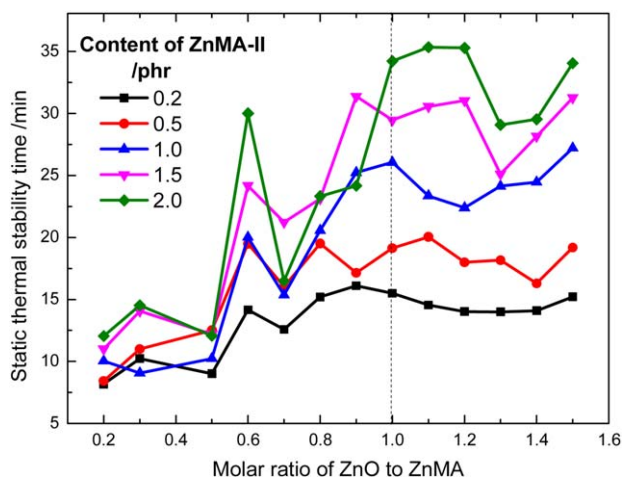


Figure 2. Effect of molar ratio of ZnO to ZnMA on static thermal stability for PVC with ZnMA-II. [Color figure can be viewed in the online issue, which is available at wileyonlinelibrary.com.]

from 0.2 to 2 in this region. Finally, the static stability time decreases with further increase in the molar ratio. These results indicated that the appropriate excess of ZnO could be helpful to enhance the thermal stability of the PVC/ZnMA-I samples. It was speculated that probably highly efficient complexes were formed in the region of the molar ratio from 1.2 to 1.5. In order to prove the above mentioned prediction, the ZnMA/ZnO complex with the molar ratio of 1.2 (denoted as ZnMA-I-1.2) was selected for chemical structure analysis and mechanism discussion.

For comparison, mixtures of ZnMA and ZnO with different molar ratios were prepared by direct mixing. Their effect on thermal stability of PVC was also evaluated by congo red method. Figure 2 shows the effect of the molar ratio of ZnO to ZnMA on the static stability time of the PVC/ZnMA-II samples. The static stability time first increases with the increase in molar ratio, and then acquires a high level value at the molar ratio of 1.0 (The mixture with the molar ratio of 1.0 was denoted as ZnMA-II-1.0). The values of stability time remain constant with further increase in the molar ratio. These maintained values were different for PVC with different amount of ZnMA-II stabilizer. For example, the static stability time for the PVC/ZnMA-II-1.0 increased from about 15.5 min to 34.7 min when the amount of ZnMA-II-1.0 increased from 0.2 to 2.0. The results indicated that ZnO and ZnMA exhibited a good synergistic effect on thermal stability of PVC. The molar ratio of ZnO and ZnMA played an important role in this synergistic effect. The ZnMA-II-1.0 mixture exhibited the best thermal stabilizing effect on PVC. The synergistic effect of ZnO and ZnMA were discussed for PVC/ZnMA-II-1.0 samples as well as their thermal stability mechanism were investigated.

In order to confirm the optimal thermal stability of PVC with ZnMA-I-1.2 and ZnMA-II-1.0 stabilizers, the static and dynamic thermal stability test were conducted to further evaluate the stability of the samples with different amounts of the stabilizers. Figure 3 exhibits the static stability time of the samples. The stability time of PVC is significantly enhanced by ZnMA-I-1.2 or ZnMA-II-1.0 stabilizers compared to ZnMA and ZnO. The

improvement in thermal stability becomes obvious with increasing amount of the stabilizers. The thermal stability time of PVC with 2.0 phr ZnMA-I-1.2 or ZnMA-II-1.0 (phr is parts by weight per hundred parts of resin) is two times higher than that of PVC with 2.0 phr ZnMA or ZnO. The results indicated that ZnMA and ZnO exhibited excellent synergistic effect. Furthermore, the PVC/ZnMA-II-1.0 samples exhibited better static thermal stability than that of the PVC/ZnMA-I-1.2 samples, which indicated the formation of different complex structures in different methods.

Figure 4 shows the weight loss and differential thermal gravity (DTG) curves of pure PVC and PVC mixed with ZnMA-I-1.2 or ZnMA-II-1.0 under nitrogen flow. The results indicate that the thermal decomposition of PVC, PVC/ZnMA-I-1.2, and PVC/ZnMA-II-1.0 samples can be divided into two stages. In the first stage, the thermal decomposition mainly involves the evolution of hydrogen chloride and formation of conjugated polyene sequences. In the second stage, the thermal decomposition primarily involves the cyclization of conjugated polyene sequences to form aromatic compounds.^{20–23} Table I lists the values of weight loss and onset decomposition temperatures for the samples. The incorporation of ZnMA-I-1.2 (or ZnMA-II-1.0) in PVC obviously increased the thermal decomposition temperature in both stages and reduced the maximal weight loss rate when the content of the stabilizer was 2.0 phr. For pure PVC, the rapid weight loss rate was observed at 270°C at the first stage; however, the rapid weight loss rate was at 440°C at the second stage. However, for the PVC/ZnMA-I-1.2 samples, the rapid weight loss rate was observed at 316°C at the first stage and 476°C at the second stage. The char residue of PVC also increased in the presence of ZnMA-I-1.2. These results indicated that ZnMA-I-1.2 could retard the dehydrochlorination of PVC at the first stage and also suspend the cyclization of conjugated polyene sequences at the second stage. Similar improvement in thermal stability was observed in PVC incorporated with ZnMA-II-1.0, which indicated that ZnMA-II-1.0 exhibited similar stabilization mechanism to ZnMA-I-1.2.

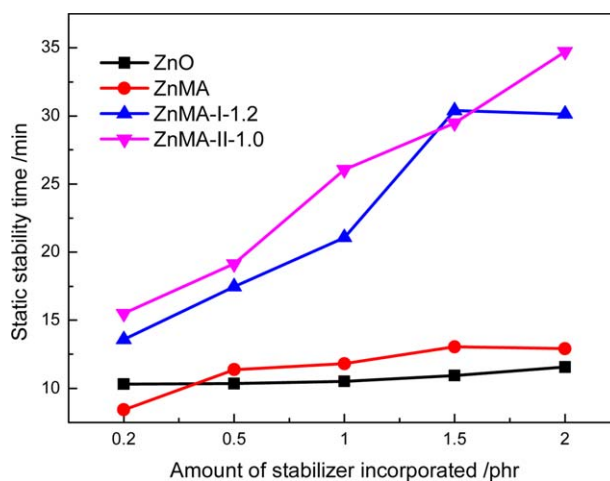


Figure 3. Comparison of different stabilizers on the static stability time of the PVC/stabilizer samples. [Color figure can be viewed in the online issue, which is available at wileyonlinelibrary.com.]

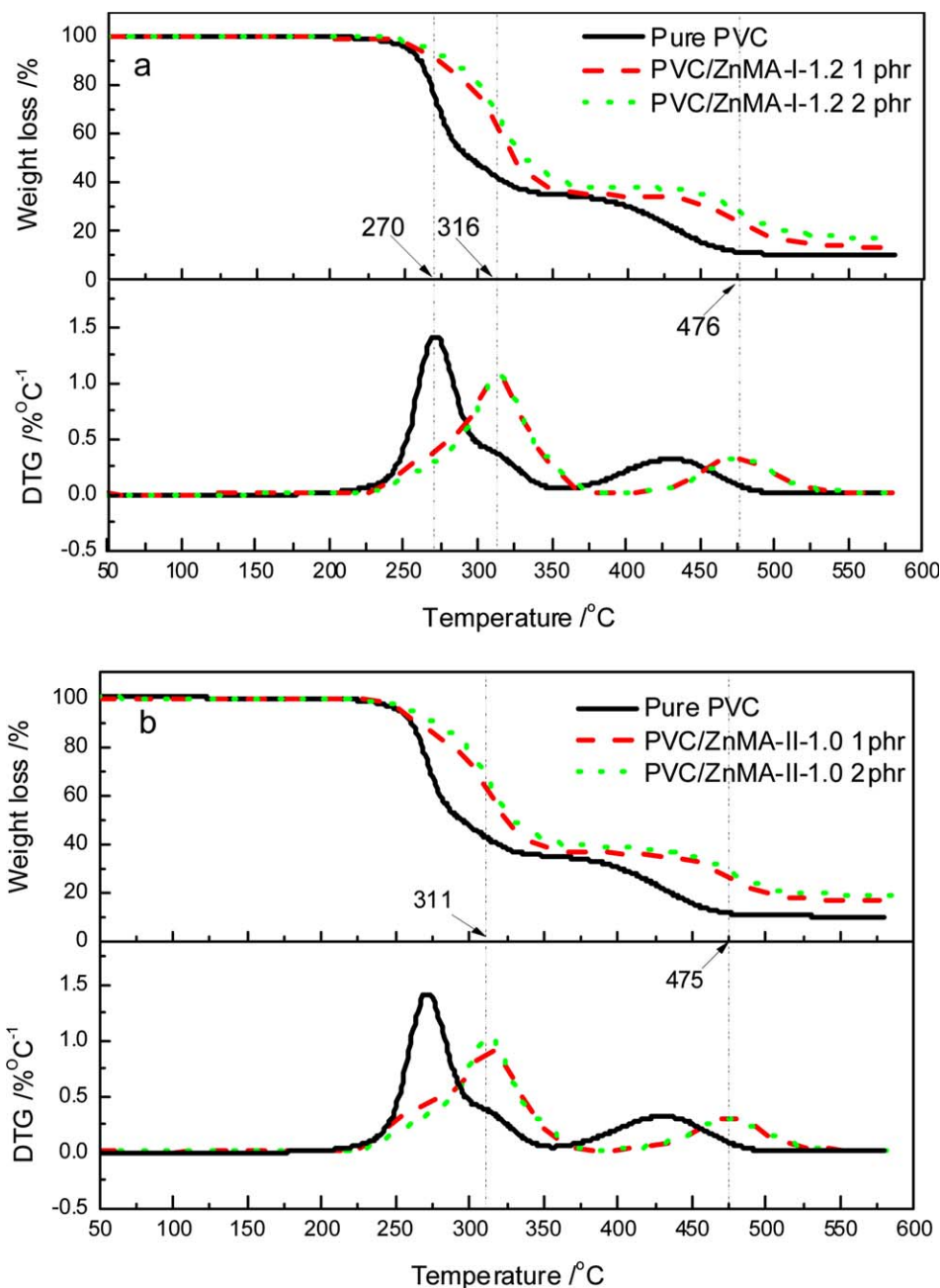


Figure 4. TG-DTG curves of PVC, PVC/ZnMA-I-1.2 samples (a), and PVC/ZnMA-II-1.0 samples (b). [Color figure can be viewed in the online issue, which is available at wileyonlinelibrary.com.]

The dynamic stability time with shear (30 rpm) of PVC with the stabilizers was obtained by a Brabender plastograph (Plasticorder) mixer at 180°C. The values of dynamic stability time of the PVC/stabilizer samples are listed in Table II. The dynamic stability time of PVC stabilized with ZnMA-I-1.2 or ZnMA-II-1.0 is longer than that of the PVC/ZnMA samples at the same loading. PVC with ZnMA-I-1.2 exhibited slightly better thermal stability than that of PVC with ZnMA-II-1.0. The dynamic stability time further increased for the PVC/ZnMA-I-1.2 or PVC/ZnMA-II-1.0 samples in presence of CaSt₂, which indicated excellent synergistic effect between ZnMA-I-1.2 and CaSt₂, or ZnMA-II-1.0 and CaSt₂.

Complex Structure in ZnMA-I-1.2 and ZnMA-II-1.0

Figure 5 exhibits the XRD spectra of pure ZnMA, ZnO, ZnMA-I-1.2, and ZnMA-II-1.0. Our previous study revealed that the structure of ZnMA was composed of Zn(C₄H₃O₄)₂ and ZnC₄H₂O₄. The diffraction peaks of ZnMA at 13.5, 17.6, and 24.4° are the characteristic peaks of Zn(C₄H₃O₄)₂; however, the peaks at 10.9, 16.9, 20.9, 22.7, and 31.2° are the characteristic peaks of ZnC₄H₂O₄.¹⁹ However, interestingly, the characteristic peaks of ZnMA and ZnO are not observed in the spectra of ZnMA-I-1.2 and ZnMA-II-1.0, indicating the formation of different crystalline structures in ZnMA-I-1.2 and ZnMA-II-1.0. The characteristic peaks of ZnMA-I-1.2 and ZnMA-II-1.0 are

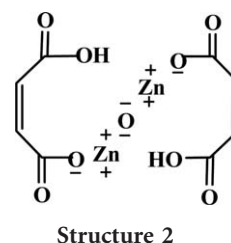
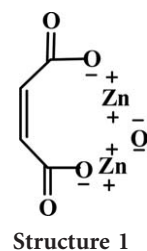
Table I. TGA Results of PVC, PVC/ZnMA-I-1.2, and PVC/ ZnMA-II-1.0 Samples

Stages	PVC	PVC/ZnMA-I-1.2 1.0 phr	PVC/ZnMA-I-1.2 2.0 phr	PVC/ZnMA-II-1.0 1.0 phr	PVC/ZnMA-II-1.0 2.0 phr
First stage					
Onset (°C)	236	243	247	241	242
Inflection (°C)	271	314	316	314	311
Completion (°C)	340	362	367	363	364
Weight loss (%)	64	64	60	63	60
Max weight loss rate (%/min)	18.6	12.8	12.8	10.2	13.4
Second stage					
Onset (°C)	391	446	450	442	443
Inflection (°C)	440	476	476	475	475
Completion(°C)	508	551	562	557	556
Weight loss (%)	25	22	22	20	22
Max weight loss rate (%/min)	3.5	3.4	3.4	3.3	3.1
Char residue (%)	11	14	18	17	18

observed at 9.7 and 26.7°, respectively. The compound could be easily formed between Zn^{2+} and MA^{2-} (or MAH^{-})²⁴; therefore, it was imagined that ZnO and ZnMA could form structure 1 and structure 2 in ZnMA-I-1.2 and ZnMA-II-1.0 according to the structures of ZnMA.¹⁹

In order to confirm our presumption, the FTIR and TGA were conducted for ZnMA-I-1.2 and ZnMA-II-1.0. According to the literature, the value of $\Delta\nu_{as-s}$ (difference in frequency separation between the COO^{-} asymmetric and symmetric stretches) provides information about the coordination between metal ion(s) and carboxylic groups. There are three representative types of coordination of the carboxylate (COO^{-}) group to metal ion(s), such as unidentate, bidentate, and bridging. The empirical rule was expressed as $\Delta\nu_{as-s}(\text{unidentate}) > \Delta\nu_{as-s}(\text{ionic}) \sim \nu_{as-s}(\text{bridging}) > \Delta\nu_{as-s}(\text{bidentate})$.²⁵ Figure 6 shows the FTIR spectra of pure ZnMA, ZnMA-I-1.2, and ZnMA-II-1.0. A broad peak from 2500 to 3600 cm^{-1} observed in the spectra of all samples indicates the presence of hydroxyl ($-OH$) groups in the structures of the samples. A characteristic peak of 460 cm^{-1} is

observed in both ZnMA-I-1.2 and ZnMA-II-1.0, indicating the existence of Zn–O bonds in the samples. The $\Delta\nu_{as-s}$ of ZnMA-I-1.2 and ZnMA-II-1.0 are 170 and 144 cm^{-1} , respectively, higher than the $\Delta\nu_{as-s}$ of MAH (140 cm^{-1}).¹⁹ The COO^{-} group in MAH could be treated as the type of ionic coordination. The results revealed that Zn ions mainly formed the unidentate structure with COO^{-} in ZnMA-I-1.2 and ZnMA-II-1.0, such as structure 1 and structure 2.

**Table II.** Dynamic Stabilization Time of the PVC/Stabilizer Samples

Formulation	Dynamic stabilization time/min
PVC/2.5phr ZnMA-I-1.2/2.5phr CaSt ₂	9
PVC/2.5phr ZnMA-II-1.0/2.5phr CaSt ₂	10
PVC/2.5phr ZnMA/2.5phr CaSt ₂	8
PVC/2.5phr ZnMA	4
PVC/5.0phr ZnMA	5
PVC/2.5phr ZnMA-I-1.2	5
PVC/5.0phr ZnMA-I-1.2	6
PVC/2.5phr ZnMA-II-1.0	4
PVC/5.0phr ZnMA-II-1.0	5

The thermal decomposition of ZnMA involved several decomposing steps, including dehydration, anion decomposition, and the final residue was ZnO.^{26,27} Figure 7 shows the weight loss and simultaneous DTG curves of ZnMA-I-1.2 and ZnMA-II-1.0. For ZnMA-I-1.2, four main peaks in the DTG curve are observed with maxima at 77, 161, 350, and 442°C, respectively. Decomposition of ZnMA-I-1.2 included two stages with 22 and 51% weight loss, respectively. The residue weight percentage was 49%. According to these results, decomposition of ZnMA-I-1.2 could be represented by Scheme 1. The molar ratio of the structure 1 and structure 2 was 1 : 2 which was calculated from

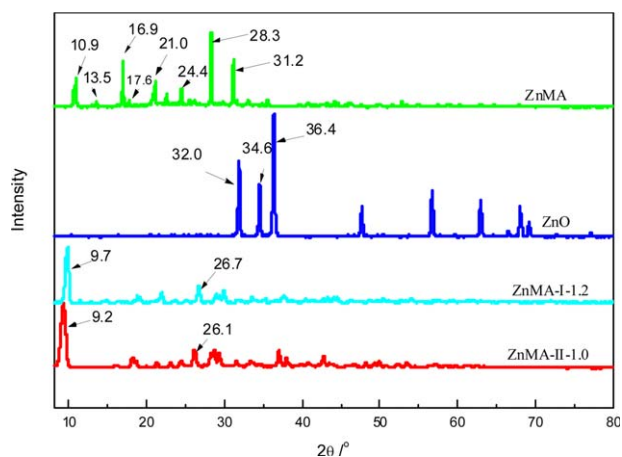


Figure 5. X-ray diffraction spectra of ZnMA, ZnO, ZnMA-I-1.2, and ZnMA-II-1.0. [Color figure can be viewed in the online issue, which is available at wileyonlinelibrary.com.]

the TGA data. The initial step in the thermal decomposition was the decomposition of structure 2 into structure 1 which was followed by the decomposition of structure 1.

For ZnMA-II-1.0, three main peaks are observed in the DTG curve with maxima at 94, 350, and 442°C, respectively. The decomposition included two stages with 14 and 41% weight loss. Our previous study revealed that the structure of ZnMA was composed of $\text{ZnC}_4\text{H}_2\text{O}_4$ and $\text{Zn}(\text{C}_4\text{H}_3\text{O}_4)_2$ in the ratio of 5 : 3. The molar ratio of ZnMA and ZnO was 1 : 1. Therefore, it could be deduced that the structure was composed of structures 1 and 2 with the molar ratio of 5 : 3. The molar ratio of the structure 1 and structure 2 could also be calculated from the TGA data. The investigation of thermal decomposition revealed that structure 2 decomposed first which was followed by the decomposition of structure 1, as shown in Scheme 2. The results indicated that both the ZnMA-I-1.2 and ZnMA-II-1.0 were composed of structures 1 and 2; however, with different molar ratios.

Thermal Stabilization Mechanism of ZnMA-I-1.2 and ZnMA-II-1.0

The results of the congo red test (Figure 3), TGA (Figure 4), and dynamic stability study (Table I) indicated that the thermal stability of PVC was significantly enhanced by ZnMA-I-1.2 or ZnMA-II-1.0. The static and dynamic stability results illustrated that the “zinc burning” effect was suppressed by ZnMA-I-1.2 or ZnMA-II-1.0. The TGA results showed that ZnMA-I-1.2 or ZnMA-II-1.0 retarded the dehydrochlorination of PVC at the first stage and also suspended the cyclization of conjugated polyene sequences at the second stage. According to the improved stabilization behavior and our previous study on ZnMA, the thermal stabilization mechanism of ZnMA-I-1.2 and ZnMA-II-1.0 could be explained as follows: the structures 1 and 2 in ZnMA-I-1.2 or ZnMA-II-1.0 (I) replaced the labile chlorine atoms (Schemes 3 and 4), (II) interrupted the formation of conjugated double bonds in PVC chains (Schemes 5 and 6) via Diels–Alder reaction, and (III) acted as the absorber of HCl to restrain the self-catalytic dehydrochlorination (Schemes 3 and 4).

In order to confirm the stabilization mechanism of ZnMA-I-1.2 and ZnMA-II-1.0, the PVC/2.0 phr ZnMA-I-1.2 and PVC/2.0 phr ZnMA-II-1.0 samples after degradation at 180°C for different times were investigated by gel content and color analyses, and also by FTIR and UV–Vis spectroscopy. According to the literature, crosslinking polyene is observed in the PVC/ ZnSt_2 and PVC/ZnMA mixture which results in the formation of gel, due to the effect of ZnCl_2 and the Diels–Alder reaction between ZnMA and polyene formed in degraded PVC chains.^{10,19} The gel content analysis of ZnMA-I-1.2 and ZnMA-II-1.0 was also performed to study the crosslinking effect of the stabilizers. The inset tables in Figure 8 exhibit the gel content of the PVC/2.0 phr ZnMA-I-1.2 and PVC/2.0 phr ZnMA-II-1.0 samples with different degradation time. The gel content of the PVC/2.0 phr ZnMA-I-1.2 samples reached 29% on heating for only 2 min and increased with increase in heating time, indicating that the crosslinking reactions between PVC chains and ZnMA-I-1.2 probably occurred at the very beginning stage. Similar behavior was observed in the PVC/2.0 phr ZnMA-II-1.0 samples. The contribution to the gel content of the PVC samples incorporated with ZnMA-I-1.2 and ZnMA-II-1.0 resulted not only from the effect of Zn^{2+} , but also from the Diels–Alder reaction.

The crosslinked chains were easily formed in the PVC samples incorporated with ZnMA-I-1.2 and ZnMA-II-1.0; therefore, it was extremely difficult to compare the UV–Vis spectral results, owing to different concentrations of the soluble portion. Therefore, the samples were dissolved in THF by ultrasonication prior to the UV–Vis test. All the degraded samples dispersed well in THF after 10 min of ultrasonic treatment. Although some polymer chains might have been broken by the ultrasonic waves, this process had negligible influence on the results of the UV–Vis spectroscopy. The UV–Vis curves of the PVC/2.0 phr ZnMA-I-1.2 samples with different heating time are shown in Figure 8(a). The samples without heating were also tested for comparison. The maximum absorption wavelength of the unheated samples was ca. 220 nm which was probably related to the $n\text{-}\sigma^*$ absorption of PVC chains. The maximum absorption wavelength of the samples after heating was about 250 nm, which

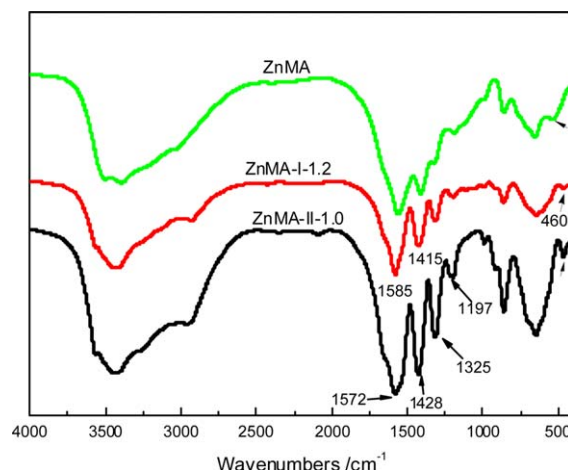


Figure 6. FTIR spectra of ZnMA, ZnMA-I-1.2, and ZnMA-II-1.0. [Color figure can be viewed in the online issue, which is available at wileyonlinelibrary.com.]

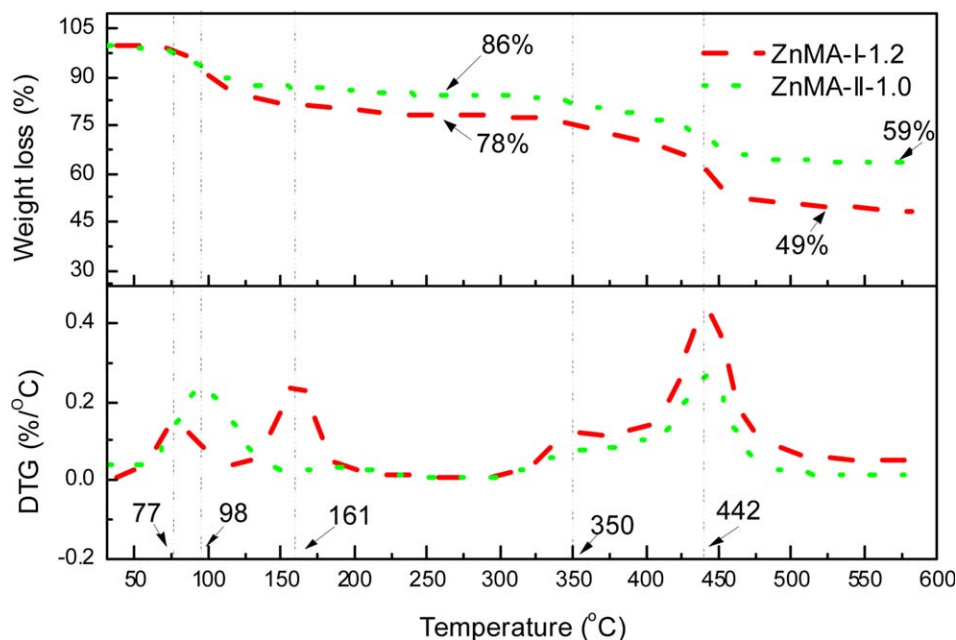
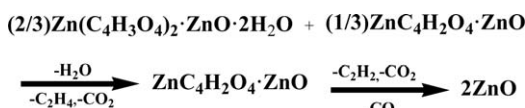


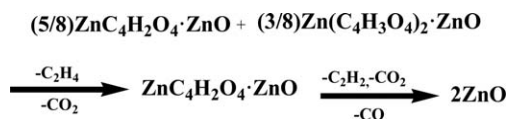
Figure 7. TG and DTG curves of ZnMA-I-1.2 and ZnMA-II-1.0 in nitrogen atmosphere. [Color figure can be viewed in the online issue, which is available at wileyonlinelibrary.com.]

was attributed to the π - π^* absorption of three conjugated double bonds in PVC chains. The results indicated that the main product of degradation was probably the three conjugated double bonds. Furthermore, the absorption at the higher wavelength also increased, but slowly, with the increase in heating time compared to pure PVC.²⁸ The amount of polyene sequences calculated by integrating the curves also increased gradually with the degradation time, as shown in the table in Figure 8(a). These results indicated that the ZnMA-I-1.2 was highly efficient in retarding the formation of polyene sequences, in particular, for the degradation time below 9 min. The investigation of the color change of the PVC samples incorporated with ZnMA-I-1.2 also reveals that the color stability is significantly improved and the “zinc burning” is completely retarded, as shown in Figure 8(a).

Figure 8(b) depicts the UV-Vis curves of the PVC samples with ZnMA-II-1.0 under different degraded time. Similar results were observed in the PVC samples with ZnMA-II-1.0. Incorporation of ZnMA-II-1.0 not only improved the color stability of PVC, but also prevented the polyene formation and “zinc burning.”



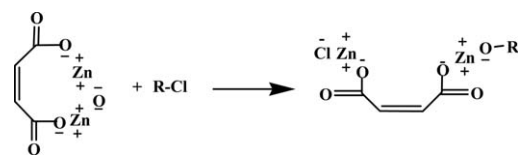
Scheme 1. Schematic representation of thermal decomposition of ZnMA-I-1.2.



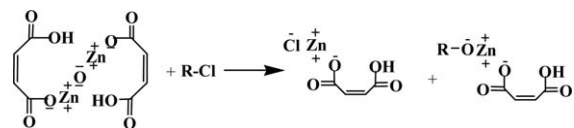
Scheme 2. Process of thermal decomposition of ZnMA-II-1.0.

However, the color of the samples containing ZnMA-II-1.0 was darkened compared to the samples with ZnMA-I-1.2. The amount of polyene in the PVC samples with ZnMA-II-1.0 was also higher than that of ZnMA-I-1.2. The results indicated that ZnMA-I-1.2 was more effective in retarding the formation of polyene sequences than ZnMA-II-1.0. Thus, the structure 2 exhibited higher color stability than structure 1.

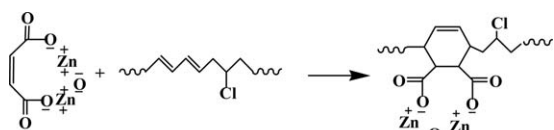
Figure 9 exhibits the FTIR spectra of the soluble part of the degraded PVC/ZnMA-I-1.2 and PVC/ZnMA-II-1.0 samples at different degradation time. The samples were prepared by dissolving in THF, filtering, and precipitating the soluble part in deionized water to remove the unreacted ZnMA-I-1.2 or ZnMA-II-1.0. Subsequently, the precipitate was dissolved again in THF, and finally cast into films for testing. The results showed the absence of characteristic peaks of ZnMA-I-1.2 and ZnMA-II-1.0 from all the spectra. There were probably two reasons to explain these results. First, if the structures 1 and 2



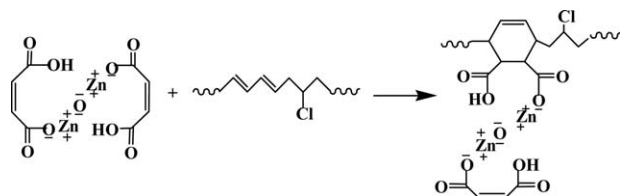
Scheme 3. Replacement of labile chlorines or HCl absorption for structure 1. (R-Cl represents hydrogen atom or a PVC chain; Cl represents a labile chlorine atom. These definitions also apply to the following schemes).



Scheme 4. Replacement of labile chlorines or HCl absorption for structure 2.



Scheme 5. Diels–Alder reaction between structure 1 and polyene.



Scheme 6. Diels–Alder reaction between structure 2 and polyene.

acted as the replacement for the labile chlorine atoms and the HCl absorption agents, their products probably were soluble in water. Second, when the Diels–Alder reaction occurred between the PVC chains and structure 1 or structure 2, the final products would be crosslinked into the insoluble part.

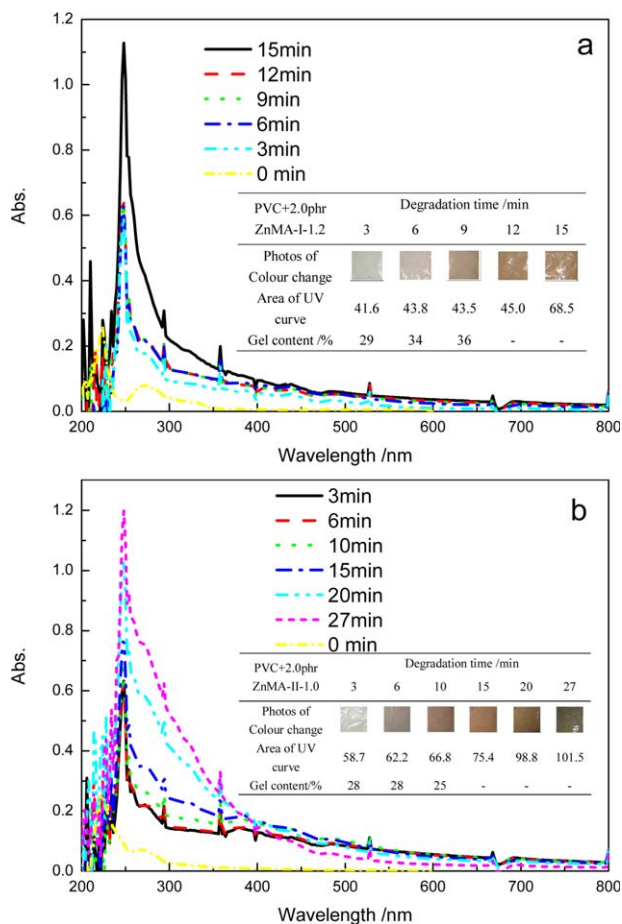


Figure 8. UV–Vis curves of the PVC/2.0 phr ZnMA-I-1.2 samples (a) and the PVC/2.0 phr ZnMA-II-1.0 samples (b) with different degradation time at 180°C. The inset tables are the color change, the area of UV-Vis curves, and gel content of the PVC/ZnMA-I-1.2 samples and the PVC/ZnMA-II-1.0 samples with different heating time. [Color figure can be viewed in the online issue, which is available at wileyonlinelibrary.com.]

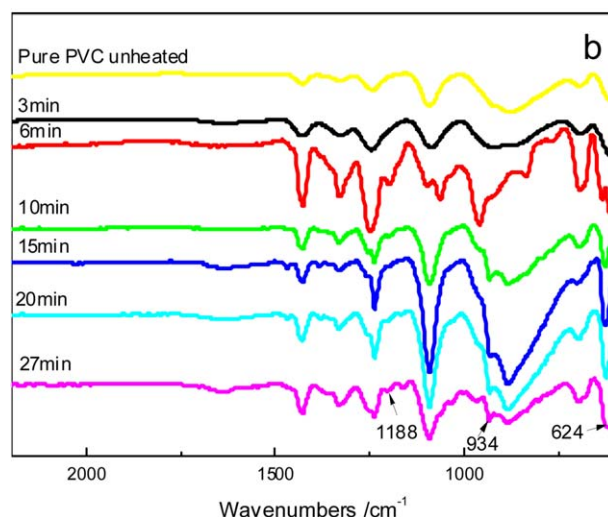
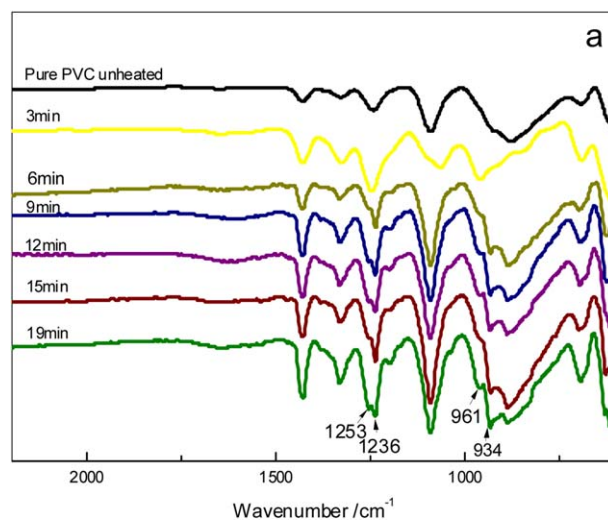


Figure 9. FTIR spectra of the soluble part of pure PVC, the degraded PVC/2.0 phr ZnMA-I-1.2 samples (a), and the degraded PVC/2.0 phr ZnMA-II-1.0 samples (b). [Color figure can be viewed in the online issue, which is available at wileyonlinelibrary.com.]

CONCLUSION

ZnMA and ZnO exhibited enhanced synergistic effect on thermal and color stability of PVC due to the formation of complex structures. There were probably two complexes formed in the directly mixed ZnO/ZnMA samples and the samples prepared by reacting MAH with excess ZnO. The optimal molar ratio of ZnO/ZnMA and ZnO/MAH for providing excellent PVC thermal stability was 1 : 1 and 1.2 : 1, respectively. The complexes exhibited two times longer PVC stability time compared to ZnSt₂ or ZnMA. They also exhibited better synergistic effect with CaSt₂ than that with ZnSt₂ or ZnMA. It was attributed to the fact that the complexes could easily replace the labile chlorine atoms, absorb hydrogen chloride, and decrease the number of conjugated double bonds via Diels–Alder reaction. The crosslinking reaction occurred in the PVC incorporated with the complexes because of the Diels–Alder reaction.

ACKNOWLEDGMENTS

The authors are grateful to the National Natural Science Foundation of China (51103119) and the Fundamental Research Funds for the Central Universities (XDJK2012C009, XDJK2014B033) for the financial support.

REFERENCES

1. Gong, F. L.; Feng, M.; Zhao, C. G.; Zhang, S. M.; Yang, M. S. *Polym. Degrad. Stabil.* **2004**, *84*, 289.
2. Wang, M.; Xu, J. Y.; Wu, H.; Guo, S. Y. *Polym. Degrad. Stabil.* **2006**, *91*, 2101.
3. Kalouskova, R.; Novotna, M.; Vymazal, Z. *Polym. Degrad. Stabil.* **2004**, *85*, 903.
4. Arkis, E.; Balkose, D. *Polym. Degrad. Stabil.* **2005**, *88*, 46.
5. Liu, Y. B.; Liu, W. Q.; Hou, M. H. *Polym. Degrad. Stabil.* **2007**, *92*, 1565.
6. Fang, L.; Song, Y.; Zhu, X.; Zheng, Q. *Polym. Degrad. Stabil.* **2009**, *94*, 845.
7. Li, M.; Jiang, Z. Y.; Liu, Z. G.; Hu, Y. H.; Wang, M. T.; Wang, H. O. *Polym. Eng. Sci.* **2013**, *53*, 1706.
8. Xu, X. P.; Chen, S.; Tang, W.; Qu, Y. J.; Wang, X. *Polym. Degrad. Stabil.* **2013**, *98*, 659.
9. Charles, E. W.; James, W. S.; Charles, A. D. *PVC Handbook*; Carl Hans Verlag, Munich, **2005**, p 95–166.
10. Wang, M.; Li, H. X.; Tang, X.; Huang, X. L. *J. Elastom. Plast.* **2013**, *45*, 173.
11. Frye, A. H.; Horst, R. W. *J. Polym. Sci.* **1959**, *40*, 419.
12. Benavides, R.; Edge, M. *Polym. Degrad. Stabil.* **1994**, *44*, 375.
13. Li, S. M.; Yao, Y. W. *Polym. Degrad. Stabil.* **2011**, *96*, 637.
14. Xu, S. L.; Li, D. G.; Yu, X. J.; Zhang, Y. L.; Yu, Y. Z.; Zhou, M.; Tang, S. Y. *J. Appl. Polym. Sci.* **2012**, *126*, 569.
15. Xu, X. P.; Chen, S.; Tang, W.; Qu, Y. J.; Wang, X. *Polym. Degrad. Stabil.* **2014**, *99*, 211.
16. Jiang, P. P.; Song, Y. Y.; Dong, Y. M.; Yan, C. R.; Liu, P. J. *J. Appl. Polym. Sci.* **2013**, *127*, 3681.
17. Fang, Y. Q.; Wang, Q. W.; Guo, C. G.; Song, Y. M.; Cooper, P. A. *J. Anal. Appl. Pyrol.* **2013**, *100*, 230.
18. Liu, Y. B.; Liu, W. Q.; Hou, M. H. *Polym. Degrad. Stabil.* **2007**, *92*, 1565.
19. Wang, M.; Li, H. X.; Huang, X. L.; Yi, L. *J. Vinyl Addit. Techn.* **2014**, *20*, 1.
20. Jimenez, A.; Berenguer, L. J.; Sanchez, A. *J. Appl. Polym. Sci.* **1993**, *50*, 1565.
21. Montrikool, O.; Wootthikanokkhan, J.; Meeyoo, V. *J. Anal. Appl. Pyrol.* **2005**, *73*, 77.
22. Gonzalez, N.; Mugica, A.; Fernandez-Berridi, M. J. *Polym. Degrad. Stabil.* **2006**, *91*, 629.
23. Yoshioka, T.; Akama, T.; Uchida, M.; Okuwaki, A. *Chem. Lett.* **2000**, *29*, 322.
24. Bychkova, S. A.; Katrovtseva, A. V.; Kozlovskii, E. V. *Russ. J. Coord. Chem.* **2008**, *34*, 93.
25. Deacon, G. B.; Phillips, R. *J. Coord. Chem. Rev.* **1980**, *33*, 227.
26. Gabal, M. A. *Thermochim. Acta* **2003**, *402*, 199.
27. Nikumbh, A.; Pardeshi, S.; Raste, M. *Thermochim. Acta* **2001**, *374*, 115.
28. Khan, W.; Ahmad, Z. *Polym. Degrad. Stabil.* **1996**, *53*, 243.